A MECHANISTIC STUDY OF ANODIC FORMATION OF POROUS InP

C. O'Dwyer[†‡], D. N. Buckley[†‡], D. Sutton[‡], M. Serantoni[‡]
and S. B. Newcomb[‡]

[†] *Dept. of Physics, University of Limerick, Ireland*
[‡] *Materials and Surface Science Institute, University of Limerick, Ireland*

ABSTRACT

When porous InP is anodically formed in KOH electrolytes, a thin layer ~40 nm in thickness, close to the surface, appears to be unmodified. We have investigated the earlier stages of the anodic formation of porous InP in 5 mol dm^{-3} KOH. TEM clearly shows individual porous domains which appear triangular in cross-section and square in plan view. The cross-sections also show that the domains are separated from the surface by a ~40 nm thick, dense InP layer. It is concluded that the porous domains have a square-based pyramidal shape and that each one develops from an individual surface pit which forms a channel through this near-surface layer. We suggest that the pyramidal structure arises as a result of preferential pore propagation along the <100> directions. AFM measurements show that the density of surface pits increases with time. Each of these pits acts as a source for a pyramidal porous domain, and these domains eventually form a continuous porous layer. This implies that the development of porous domains beneath the surface is also progressive in nature. Evidence for this was seen in plan view TEM images. Merging of domains continues to occur at potentials more anodic than the peak potential, where the current is observed to decrease. When the domains grow, the current density increases correspondingly. Eventually, domains meet, the interface between the porous and bulk InP becomes relatively flat and its total effective surface area decreases resulting in a decrease in the current density. Quantitative models of this process are being developed.

INTRODUCTION

There is considerable interest in the electrochemical formation of porosity in semiconductors, both from the point of view of fundamental understanding and their application.[1-7] Much of the work has focused on silicon but investigations of pore formation in III-V semiconductors such as GaAs[8-11] and InP[12-15] have also been reported. It has been suggested that controlled modulation of the pore diameter and pore growth direction in such structures could lead to photonic crystals with a photonic band gap in the near-infra red or visible region. Such parameters have been shown to be affected by electrolyte concentration[12,16,17], substrate type[18], orientation[19] and doping density.[20] Significant progress has been made in understanding the basic mechanisms of pore formation in silicon under electrochemical conditions, but only a limited number of

investigations of the mechanism of pore formation in III-V semiconductors have been reported. For silicon, several pore formation models have been proposed to account for the variety of observed pore types,[21-23] but for III-V semiconductors, no detailed models have been proposed.

A subject of interest is the preferential orientation of the pore growth along specific crystallographic directions and how this leads to the development of a complete porous region within the semiconductor. This paper presents results of a detailed investigation of the mechanism of the formation of porous InP in aqueous KOH electrolytes under anodic conditions.

EXPERIMENTAL

The working electrode consisted of polished (100)-oriented monocrystalline sulfur doped n-InP with a carrier concentration of $\sim 3 \times 10^{18}$ cm^{-3}. An ohmic contact was made by alloying indium to the InP sample and the contact was isolated from the electrolyte by means of a suitable varnish. The electrode area was typically 0.2 cm^2. Anodization was carried out in an aqueous KOH electrolyte at a concentration of 5 mol dm^{-3}. A conventional three electrode configuration was used employing a platinum counter electrode and saturated calomel reference electrode (SCE) to which all potentials are referenced. Prior to immersion in the electrolyte, the working electrode was dipped in a 3:1:1 H_2SO_4:H_2O_2:H_2O etchant and rinsed in deionized water. All of the electrochemical experiments were carried out at room temperature and in dark conditions.

A CH Instruments Model 650A Electrochemical Workstation interfaced to a Personal Computer (PC) was employed for cell parameter control and for data acquisition. Slices for plan view and cross-sectional microscopic analysis were prepared by thinning to electron transparency using standard focused ion beam milling procedures by means of a FEI 200 FIBSIMS workstation. The transmission electron microscopy (TEM) characterization was performed using a JEOL 2010 TEM operating at 200 kV.

.

RESULTS AND DISCUSSION

Fig. 1 shows the cyclic voltammetric response of an n-InP electrode in a 5 mol dm^{-3} KOH solution. The potential was scanned at a rate of 2.5 mV s^{-1} from 0.0 V to 0.68 V and back to 0.0 V. At potentials less than 0.3 V, very little current flow is observed, but continued anodization to potentials greater than 0.35 V results in a rapid increase in the current density from a value of 1 mA cm^{-2} at 0.35 V to a peak value of 20 mA cm^{-2} at 0.48 V. Above 0.48 V, the current density decreases quite rapidly, reaching a value of 3 mA cm^{-2} at 0.6 V. Clearly, a significant anodic oxidation process occurs above 0.35 V and becomes self-limiting at higher potentials. We have recently reported that such anodic processes result in the formation of a porous region below the surface of the InP electrode.[12] As can be seen from Fig. 1, the current densities on the return sweep are much lower than the corresponding current densities on the forward sweep. A similar current-voltage curve was noted by Hamamatsu et al.[24], who attributed the decrease in current density and resulting effective passivation to the presence of a surface oxide when

n-InP is anodized in a similar way in a 1 mol dm^{-3} HCl electrolyte even after porous n-InP formation had taken place.

Examination of electrode cross-sections using TEM shows that the process corresponding to the anodic current in Fig. 1 involves the formation of a porous sub-surface region. Fig. 2(a) is a TEM micrograph of a cross-section of an InP electrode after a potential sweep from 0.0 V to 0.7 V in 5 mol dm^{-3} KOH. The porous region is clearly observed to extend over 1.1 μm into the InP substrate. However, a thin layer ~40 nm in thickness close to the surface appears to be unmodified. We have observed similar behavior under both potential sweep and constant potential conditions in KOH electrolytes[12] with concentrations ranging from 2 – 5 mol dm^{-3} and in all cases a thin, dense, near-surface layer is present above the porous region. Electron diffraction measurements have shown this layer to be single crystal InP, *i.e.* unmodified electrode material.

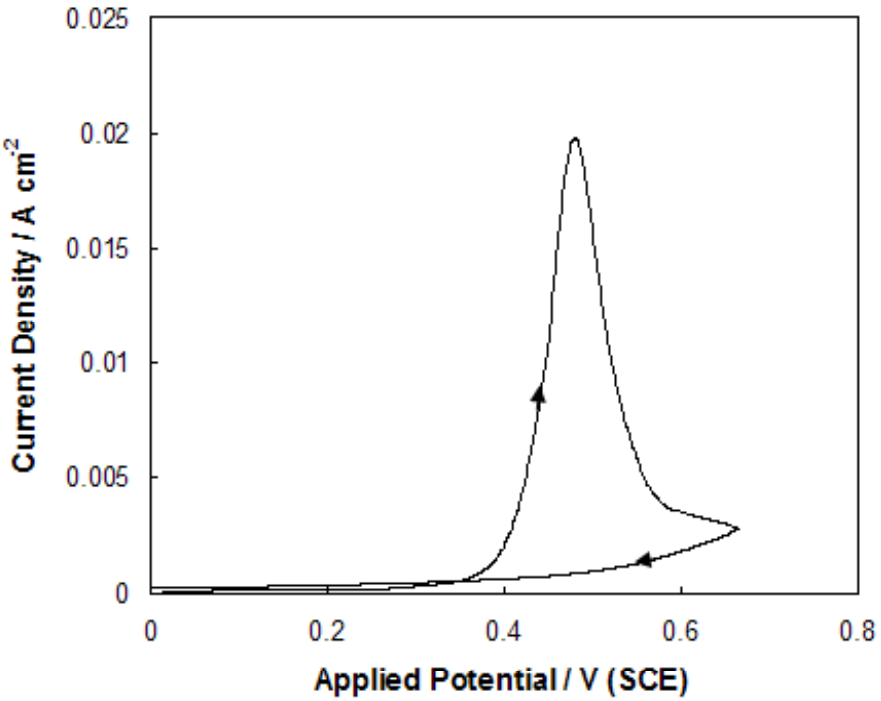

Fig. 1 Cyclic voltamogram of an n-InP electrode in a 5 mol dm^{-3} KOH electrolyte from 0.0 V to 0.68 V (SCE). The potential was scanned at a rate of 2.5 mV s^{-1}.

The mechanism by which a porous region can form by electrochemical oxidation of the substrate, despite the presence of this dense InP layer at the surface is not apparent from Fig. 2(a). Closer examination by TEM reveals that the dense, near-surface layer is penetrated at certain points by narrow channels. The TEM micrograph in Fig. 2(b) shows a typical example. This is corroborated by AFM examination of the surface. A detailed examination, using AFM, of surfaces of electrodes subjected to potential sweeps to various upper potentials has shown the progressive formation of etch pits on the surface. Typical AFM images of electrode surfaces after anodization to upper potentials of 0.44 V and 0.475 V respectively are shown in Fig. 3. Both images show a distribution of pits on the surface and it is evident that a higher density is obtained at 0.475 V as compared with

0.44 V. Based on AFM measurements, the density of etch pits at the peak potential (0.48 V) is estimated to be ~5 × 10^6 cm^{-2}. Thus, the observed density is very low compared with the porous region.

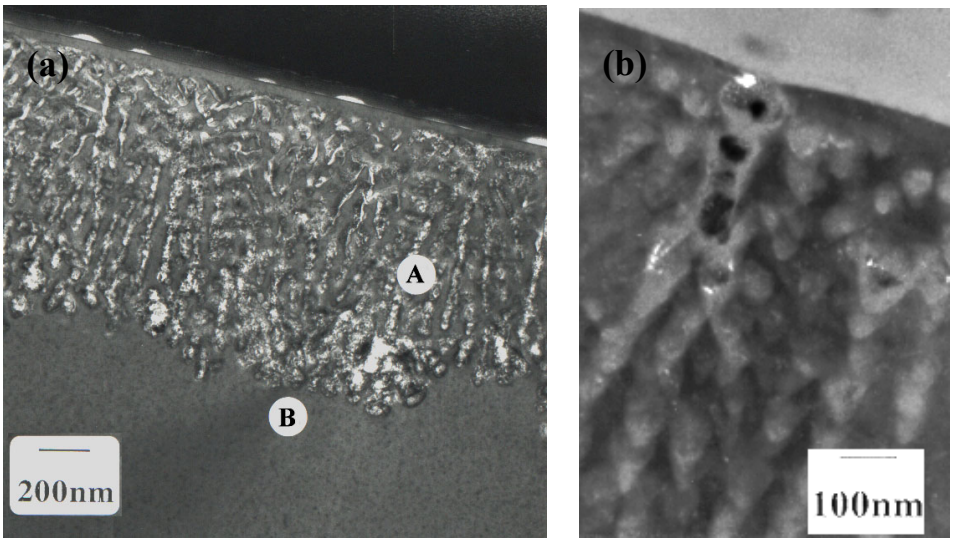

Fig. 2 Cross-sectional bright field through focal TEM of n-InP after a potential sweep from 0.0 V to 0.7 V (SCE) at a scan rate of 2.5 mV s^{-1} in 5 mol dm^{-3} KOH electrolyte. (b) Dark Field TEM of the porous InP cross-section showing a channel in the near-surface layer. The plane of the micrographs is (110).

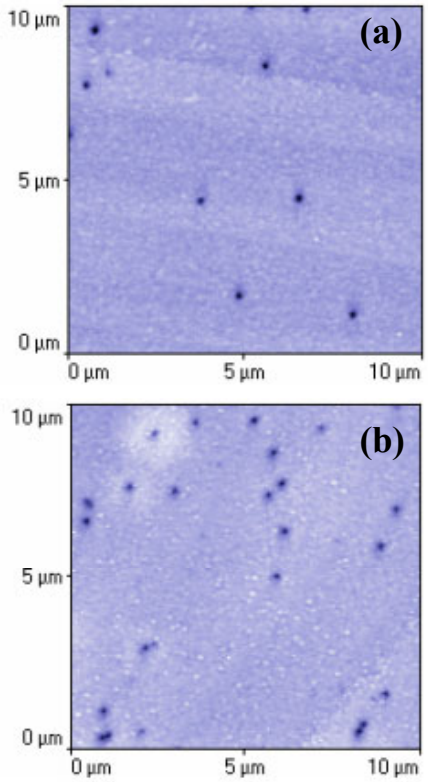

Fig. 3 AFM images of an InP electrode surface after potential sweep anodization at 2.5 mV s^{-1} from 0.0 V to (a) 0.44 V and (b) 0.475 V in a 5 mol dm^{-3} KOH electrolyte.

However, it appears that these surface pits correspond to channels which connect the porous region to the bulk electrolyte. This suggests a mechanism by which the electrochemical oxidation of InP at the pore tips, and thus porous layer growth, can continue. Both the porous layer and the channels through the near-surface layer must be filled with electrolyte. This would enable ionic current to flow and electrochemical oxidation of InP to proceed at the pore tips, thus providing a mechanism by which the porous layer can grow. Consequently, these channels have a critical role in the evolution of the porous structure.

In order to investigate the mechanism by which porosity develops in InP under anodic conditions in KOH, experiments were carried out in which the potential was swept from 0.0 V to 0.44 V (*i.e.* the potential sweep was stopped when the current reached approximately half its peak value) and the electrode was then cross-sectioned and examined. A TEM micrograph of such a cross-section is shown in Fig. 4. This reveals

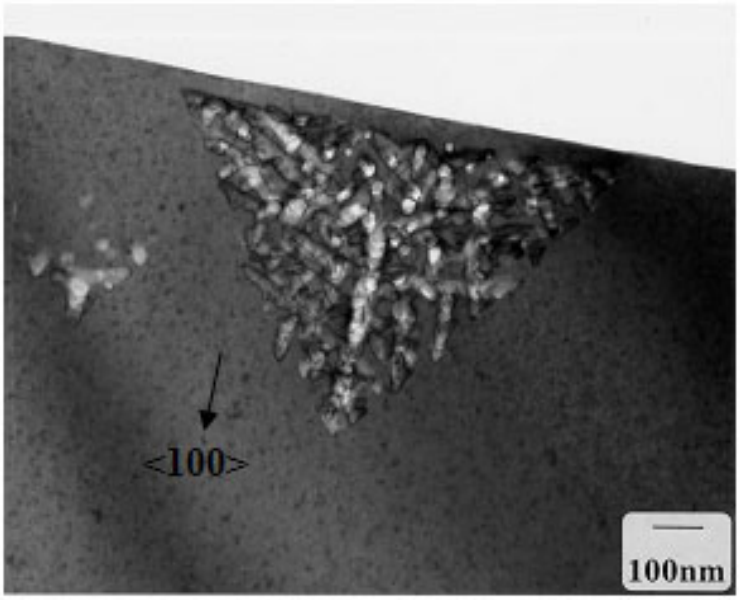

Fig. 4 Bright field TEM of a cross section of an InP electrode after a potential sweep from 0.0 to 0.44 V (SCE) in 5 mol dm^{-3} KOH at 2.5 mV s^{-1}. The plane of the micrograph is (110).

that, at this stage of the anodization, individual porous areas had formed which had a triangular cross-section with the base of the triangle parallel to the InP surface. As was observed for the more fully developed porous layer (Fig. 2) the triangular porous region is separated from the surface by a thin non-porous layer. The measured thickness of this layer in Fig. 4 is ~40 nm. The dimensions of the triangular cross-section in Fig. 4 are shown in Fig. 5. The base of the triangle measures 920 nm and the other sides are equal to each other within experimental error (2%) with a length of 800 nm. Thus, the height of the triangle is 655 nm and the angle between the base and the sides is 54.9^0.

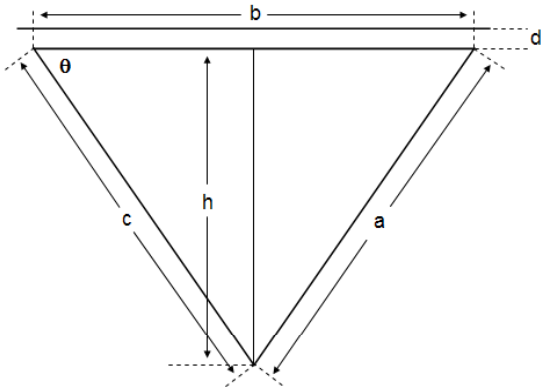

Fig. 5 Schematic representation of the triangular porous region shown in Fig. 4. The base of the triangle is a distance d = 40 nm below the surface of the InP. The length of the base is b = 920 nm, the length of the sides is $a = c$ = 800 nm and the angle between the base and side is $\theta = 54.9^0$.

The cross-section in Fig. 4 is along the (011) plane. By symmetry we would expect a similar cross-section along the perpendicular (011) plane which suggests that the porous region in Fig. 4 may have a square-based pyramidal structure. This was investigated by plan-view TEM observation of the electrode. Fig. 6 shows a TEM micrograph of a slice through the InP in the (100) plane, parallel to the surface and ~100 nm below it. A porous region with an approximately square outline is clearly visible, consistent with a square pyramidal structure for the porous region as suggested above. The sides of the square in Fig. 6 are parallel to the <100> direction and are ~800 nm in length. We suggest that each pyramidal porous structure formed corresponds to a single channel through the near-surface layer. We further suggest that the pyramidal structure arises as a result of preferential pore propagation along the <100> directions.

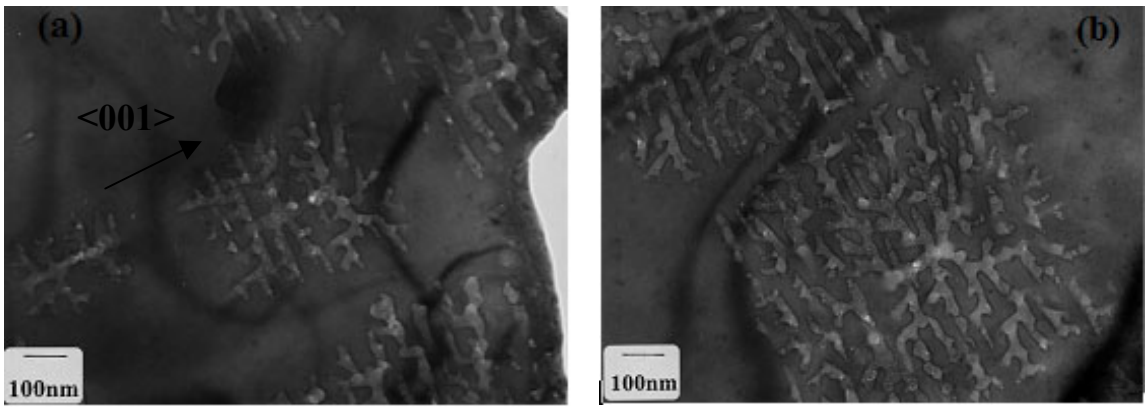

Fig. 6 Plan view bright field TEM images of a section through a porous InP layer ~100 nm below the surface of the electrode. Anodization conditions were the same as in Fig. 4. The plane of the micrograph is (100). Nearby porous domains are visible.

To facilitate discussion of the growth of an individual pyramidal porous structure, we define cartesian co-ordinates as follows. We define a *y*-axis along the [100] direction (*i.e.* normal to the surface of the electrode), an *x*-axis along the [010] direction and a *z*-axis along the [001] direction. The origin (0,0,0) is defined as the bottom of the channel through the near-surface layer. This is depicted in Fig. 7 below.

Consider a pore propagating from the origin. It can propagate in any of five directions, namely *–y, x, –x, z* and *–z*. Assume that the pore is propagating at some linear velocity *v*. If it propagates along the *–y* direction it will reach a point with co-ordinates (0, *–vt*, 0) a distance *vt* below the surface layer at time *t*. Similarly, if it propagates along the *x* direction it will reach a point (*vt*, 0, 0) just underneath the near-surface layer. If the pore propagates for time *t*/2 along the *–y* direction and then branches and travels for time *t*/2 along the *x* direction, it will reach a point (*vt*/2, *–vt*/2, 0) at time *t*. In fact, if the pore propagates along any combination of paths along the *–y* direction and the *x* direction it will reach a point on the line joining (0, *–vt*, 0) and (*vt*, 0, 0). Likewise, a pore propagating by any combination of paths along the *–y* direction and the *–x* direction will reach a point on the line joining (0, *–vt*, 0) and (*–vt*, 0, 0), at time *t*. Similarly, pores propagating along paths involving the *–y* direction in combination with the *z* direction and the *–z* direction will reach, at time *t*, points on the lines joining (0, *–vt*, 0) to (0, 0, *vt*) and (0, 0, *–vt*) respectively. Extending the argument to combinations of paths involving all three axes, it is clear that pores propagating in this way will reach, at time *t*, points on the surface of a square based pyramid defined by the above-mentioned four line segments and the plane of the bottom of the near-surface layer.

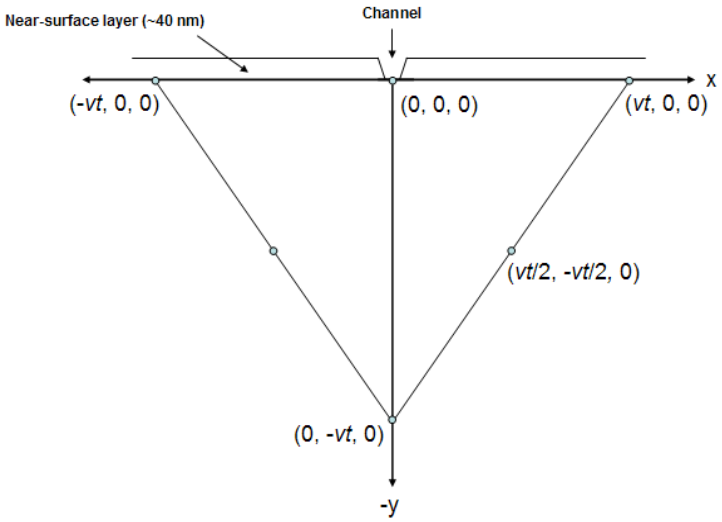

Fig. 7 Definition of cartesian co-ordinates for an individual porous region. The *y*-axis is normal to the electrode surface and the *z*-axis is out of the plane of the page. The origin is at the bottom of a channel through the near-surface layer as shown.

Anodization of InP in a 5 mol dm^{-3} KOH electrolyte at constant potentials in the range 0.5 V – 0.9 V also results in porous InP formation. Typical current-time curves exhibit a current peak: the details have been described elsewhere.[12] The porous layers observed are very similar to those obtained under potential sweep conditions, particularly

if the applied potential is in the range 0.5 – 0.7 V. As discussed earlier, AFM studies of electrodes subjected to anodic potential sweeps such as that in Fig. 1 show a distribution of pits on the surface the density of which increases progressively with increasing upper potential. Studies of the surface of electrodes subjected to constant potential anodization have shown that pits develop in a similar manner to that observed under potential sweep conditions. Estimates based on the AFM images have shown that the density of surface pits also increases with time. It is postulated, as stated earlier, that each of these pits acts as a source for a pyramidal porous domain, and these domains eventually form a continuous porous layer. This implies that the development of porous domains beneath the surface is also progressive in nature. Evidence for this can be seen in the plan view TEM images in Fig. 6. The micrographs show different areas of the same surface and it can be seen that, despite this, the porous domains in Fig. 6(a) are at an earlier stage of development than those in Fig. 6(b).

Fig. 8 shows cross-sectional TEM micrographs of an electrode subjected to anodization similar to that described for Fig. 2 except that the potential was stopped at 0.48 V (*i.e.* the peak of the current-voltage curve). Fig. 8(a) shows a relatively homogeneous porous region ~700 nm in thickness. However, Fig. 8(b) obtained at another part of the same electrode clearly shows the merging of two porous domains. This shows that, at this stage of the anodization, not all of the nucleated porous domains have fully grown and merged. Thus, merging of domains continues to occur at potentials more anodic than the peak potential, where the current is observed to decrease. When the domains grow, the current density increases correspondingly. Eventually domains meet, the interface between the porous and bulk regions of the InP becomes relatively flat and its total effective surface area decreases resulting in a decrease in the current density. Quantitative models of this process are being developed and the results will be reported elsewhere.

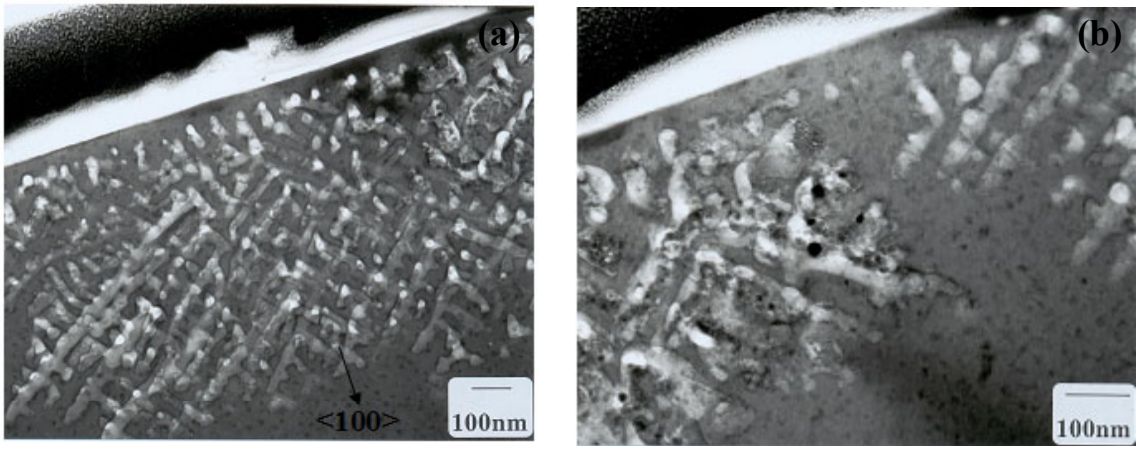

Fig. 8 (a) Cross-sectional bright field TEM of n-InP after a potential sweep from 0.0 V to 0.48 V (SCE) at a scan rate of 2.5 mV s^{-1} in 5 mol dm^{-3} KOH electrolyte. (b) TEM micrograph of a different area of the same electrode cross-section as (a) showing the merging of two porous domains. The plane of the micrographs is (110).

CONCLUSION

At the earlier stages of the anodic formation of porous InP in 5 mol dm^{-3} KOH, TEM clearly shows individual porous domains which appear triangular in cross-section and square in plan view. The cross-sections also show that the domains are separated from the surface by a ~40 nm thick, dense InP layer. It is concluded that the porous domains have a square-based pyramidal shape and that each one develops from an individual surface pit which forms a channel through this near-surface layer. We suggest that the pyramidal structure arises as a result of preferential pore propagation along the <100> directions. It is clear that pores propagating in this way with uniform velocity will reach, at a given time, points on the surface of a square-based pyramid. AFM measurements show that the density of surface pits increases with time. Each of these pits acts as a source for a pyramidal porous domain, and these domains eventually form a continuous porous layer. This implies that the development of porous domains beneath the surface is also progressive in nature. Evidence for this is seen in plan view TEM images in which domains in different areas of the same surface are seen to be at different stages of development. Merging of domains continues to occur at potentials more anodic than the peak potential, where the current is observed to decrease. When the domains grow, the current density increases correspondingly. Eventually domains meet, the interface between the porous and bulk InP becomes relatively flat and its total effective surface area decreases resulting in a decrease in the current density. Quantitative models of this process are being developed.

REFERENCES

[1] L.T. Canham, *Appl. Phys. Lett.*, **57**, 1046 (1990)
[2] H. Föll, *Appl. Phys. A*, **53**, 8 (1991)
[3] T. Holec, T. Chvojka, I. Jelínek, J. Jindřich, I. Němec, I. Pelant, J. Valenta and J. Dian, *Mater. Sci. Eng. C*, **19**, 251 (2002)
[4] R.J. Martín-Palma, J.M. Martínez-Duart, L. Li and R.A. Levy, *Mater. Sci. Eng. C,* **19**, 359 (2002)
[5] A. Matoussi, T. Boufaden, A. Missaoui, S. Guermazi, B. Bessaïs, Y. Mlik and B. El Jani, *Microelectronics Journal,* **32**, 995 (2001)
[6] A. Jain, S. Rogojevic, S. Ponoth, N. Agarwal, I. Matthew, W.N. Gill, P. Persans, M. Tomozawa, J.L. Plawsky and E. Simonyi, *Thin Solid Films,* **398**, 513 (2001)
[7] N.E. Chayen, E. Saridakis, R. El-Bahar, Y. Nemirovsky, *J. Molec. Biol.,* **312**, 591 (2001)
[8] S. Langa, J. Carstensen, M. Christophersen, H. Föll, and I.M. Tiginyanu, *Appl. Phys. Lett.*, **78**, 1074 (2001)
[9] G. Oskam, A. Natarajan, P.C. Searson and F.M. Ross, *Appl. Surf. Sci.*, **119**, 160 (1997)
[10] M.M. Faktor, D.G. Fiddyment and M.R. Taylor, *J. Electrochem. Soc.*, **122**, 1566 (1975)
[11] F.M. Ross, G. Oskam, P.C. Searson, J.M. Macaulay and J.A. Liddle, *Philos. Mag. A*, **75**, 2 (1997)
[12] C. O'Dwyer, D.N. Buckley, V.J. Cunnane, D. Sutton, M. Serantoni and S.B. Newcomb, in *Proceedings of the State-of-the-Art Program on Compound Semiconductors XXXVII*, PV 2002-14, p. 259, The Electrochemical Society, Proceedings Series, Pennington, NJ (2002)

[13] S. Langa, J. Carstensen, I.M. Tiginyanu, M. Christophersen and H. Föll, *Electrochem. Solid-State Lett.*, **4**, G50 (2001)
[14] S. Langa, I.M. Tiginyanu, J. Carstensen, M. Christophersen and H. Föll, *Electrochem. Solid-State Lett.* **3**, 514 (2000)
[15] E. Harvey, C. O'Dwyer, T. Melly, D.N. Buckley, V.J. Cunnane, D. Sutton, S.B. Newcomb and S.N.G. Chu, in *Proceedings of the 35th State-of-the-Art Program on Compound Semiconductors*, P.C. Chang, S.N.G. Chu, and D.N. Buckley, Editors, PV 2001-2, p. 87, The Electrochemical Society, Proceedings Series, Pennington, NJ (2001)
[16] P. Schmuki, J. Fraser, C.M. Vitus, M.J. Graham, H.S. Isaacs, *J. Electrochem. Soc.*, **143**, 3316 (1996)
[17] P. Schmuki, D.J. Lockwood, J. Fraser, M.J. Graham, H.S. Isaacs, *Mater. Res. Soc. Symp. Proc.,* **431**, 439 (1996)
[18] M. Christopherson, J. Carstensen, A. Feuerhake and H. Föll, *Mater. Sci. Eng. B*, **69**, 70, 194 (2000)
[19] S. Rönnebeck, J. Carstensen, S. Ottow and H. Föll, *Electrochem. Solid-State Lett.*, **2**, 126 (1999)
[20] P. Schmuki, L.E. Erickson, D.J. Lockwood, J.W. Fraser, G. Champion, H.J. Labbé, *Appl. Phys. Lett.*, **72,** 1039 (1998)
[21] B.H. Erne, D. Vanmaekelbergh and J.J. Kelly, *J. Electrochem. Soc.*, **143**, 305 (1996)
[22] J. Carstensen, M. Christophersen and H. Föll, *Mater. Sci. Eng., B*, **69-70**, 23 (2000)
[23] S. Langa, J. Carstensen, I.M. Tiginyanu, M. Christophersen and H. Föll, *Electrochem. Solid-State Lett.*, **5**, C14 (2002)
[24] K. Hamamatsu, H. Kaneshiro, H. Fujikura and H. Hasegawa, *J. Electroanal. Chem.*, **473** (1999) 223